Small-diameter ducted contrarotating propulsors for marine robots

M Jordan Stanway* and Thaddeus Stefanov-Wagner†
Center for Ocean Engineering, Department of Mechanical Engineering
Massachusetts Institute of Technology, Cambridge, MA 02139
*Email: squall@mit.edu †Email: thaddeus@alum.mit.edu

***Abstract*— Many marine robots, including industry and institution-grade systems, rely on substandard propellers for thrust. This is especially true in small systems. Many of these systems are moving toward onboard power, which is often restricted. Inefficient propulsion becomes a major design problem in these vehicles. Using computational tools, we design, test, and evaluate a small-diameter ducted contrarotating propulsor with a high thrust coefficient.**

We perform a parametric study to determine the optimum operating point and match a motor and gearbox to the propulsor. A three-dimensional vortex lattice code is then used in conjunction with a Reynolds-Averaged Navier-Stokes (RANS) flow solver to adjust the mean camber surface of the propeller blades and to determine the desired duct offsets.

The propellers and duct are manufactured using computer-numerical-controlled machines, as are the components for the motor housing and the miter gearbox used to achieve contrarotation. Propulsors are assembled for use on the MIT ROV and for testing in the recirculating water tunnel at the MIT Marine Hydrodynamics Laboratory.

Propulsion tests are conducted to determine K_T, K_Q, and η at different rotation speeds. Results show good agreement with design and modeling, with some extra losses due to manufacturing roughness and other unmodeled factors.

Propulsors were installed on the MIT ROV Team's entry into the Annual MATE ROV Competition, and performed well in real-world conditions. Lessons learned in testing and missions at the competition identified some points for future improvement in the design.

I. Introduction

There is an overall lack of purpose-designed propellers in marine robotics. Many professional and institution-grade systems rely on model airplane propellers for propulsion. In applications where space comes at a premium, having small diameter thrusters can be important. Furthermore, if these applications depend on battery power, propulsive efficiency also becomes a driving concern. Model airplane propellers do not provide satisfactory performance in these types of applications.

A pair of contrarotating propellers can provide superior thrust and efficiency at a given diameter than a single propeller [2], [6], [7]. This is partly because the load is split between both propellers, and they can therefore operate at lower speeds, which are inherently more efficient. The counter-rotating effect also cancels out the losses due to the tangential velocities, or swirl, in the propulsor wake. With this taken into account, it is possible to design a set of propellers that will function close to a pure actuator disk, providing maximum theoretical efficiency. This is especially important in systems operating at high thrust coefficients, where single propellers are further from the ideal efficiency than they are at low thrust coefficients.

Fig. 1. The ducted contrarotating propulsor, DCRP-2006, viewed from behind. The two three-bladed propellers rotate in opposite directions, canceling swirl and increasing propulsive efficiency.

II. Parametric Study

The first step in any modern propeller design cycle is a parametric study to determine the desired operating point. This is especially important for open designs that start with few hard constraints. Physical and power constraints of the vehicle are considered with the desired performance, and different values are considered for propeller diameter, rotation rate, thrust coefficient, duct loading , and number of blades. A lifting line code is used to optimize the circulation distribution around the propeller blades for each combination of the parameters under consideration. Efficiency and required torque can be determined theoretically from this information, allowing the designer to match a motor for the optimum overall design.

A. Design Requirements

The DCRP-2006 is designed for use on the MIT ROV Team's entry for the Marine Advanced Technology Education

Center's annual competition, but the thruster should be well-suited to any marine robot requiring a small-diameter, high-thrust propulsor. Since the MIT ROV uses onboard power, it is limited to 13 VDC and 25 amps. With four thrusters, these constraints on the vehicle translate to 12VDC (nominal) thrusters with a maximum continuous current of 6 amps at full speed. The MIT ROV is a small vehicle, and 11.43 cm (4.5 in) is the maximum allowable propeller diameter. These were the only constraints known at the beginning of the design.

The most important unknown variable in maximizing the efficiency of our design was the coefficient of thrust.

$$C_T = \frac{T}{\frac{1}{2}\rho U^2 \pi \frac{D^2}{4}} \tag{1}$$

Actuator disk theory shows that the maximum possible efficiency for any propulsor is a function of its thrust coefficient [1]:

$$\eta_{max} = \frac{2}{1 - \sqrt{1 - C_T}} \tag{2}$$

The thrust required from each propulsor depends on the drag that it has to overcome. In a non-dimensional comparison, it becomes apparent that this is a function of geometry, not vehicle speed[1]:

$$C_T = \frac{A_p C_D}{A_s}, \tag{3}$$

where A_p is the projected area of the vehicle, C_D is the drag coefficient based on that projected area, and A_s is the swept area of all propulsors normal to the axis of motion (for example: $A_s = \pi \frac{D^2}{4}$ per propulsor).

Having observed this, we chose a design speed of 1.03 m/s (2 knots) for the propulsors. This would enable us to complete mission tasks quickly, provide strong maneuvering authority, and allow operation of the ROV in currents of up to 1.03 m/s.

Our initial drag model for the ROV was a 30.48 cm (12 in) cube. Assuming frictional drag on the ROV is negligible compared to form drag, and using a drag coefficient of 1.05 for a square cylinder, the drag on the vehicle would be 50 N, meaning each forward propulsor would have to supply 25 N (5.6 lbf) of thrust at 1.03 m/s. With a different model based on cylinders representing many of the ROV components, the thrust required per propulsor was 20.68 N (4.65 lbf). We compared these models to simplified drag models based on the major dimensions of the Seabotix LBV [9] and Hydroid Remus [10], two popular and commercially available marine robots. The C_T required and corresponding actuator disk efficiency were calculated for the range of propeller diameters under consideration (Figure 2).

Since we wanted a generally useful propulsor, it was not immediately clear what C_T we should design for. The properties of the motor would enter the equation here, so we made an estimate of the power rating required, based on the range of efficiencies we could expect out of the propellers:

$$P = \frac{TU}{\eta_m \eta_{gb} \eta_{cr} \eta_p}, \tag{4}$$

[1]This holds true for bluff bodies and in any situation where the drag coefficient of the vehicle is a weak function of velocity.

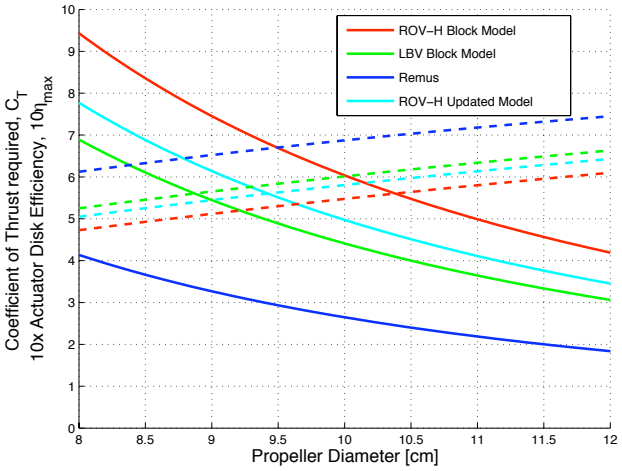

Fig. 2. Drag models for the MIT ROV (ROV-H), Seabotix LBV, and Hydroid Remus. Solid line represents the required coefficient of thrust, broken line is 10 times the actuator disk efficiency for that C_T

TABLE I

MAJOR DESIGN SPACE PARAMETERS

Parameter	range investigated	chosen value
Diameter, D [cm]	8.26-11.43	11.43
Number of blades, Z	2 - 6	3
Duct loading, τ	0.6 - 1.0	0.8
Advance coefficient, J	0.2 - 2.0	0.54

where η_m is the efficiency of the motor, η_{gb} is the efficiency of the gearbox, η_{cr} is the efficiency of the contrarotating mechanism, and η_p is the efficiency of the propellers. We assumed $0.80 < \eta_m < 0.90$, $0.80 < \eta_{gb} < 0.90$, $0.70 < \eta_{cr} < 0.80$,and $0.45 < \eta_p < 0.65$. This meant we needed a motor rated for at least 50 - 110 watts continuously. We also began exploring our design space, which was defined by four major parameters (Table I).

C_T was determined from the diameter for each testcase. The effects of duct chordlength, propeller spacing, and relative diameters of the fore and aft propellers were also studied, once a promising area of the design space was found.

B. Program Fundamentals

Propeller Lifting Line (PLL) version 4.2 is a parametric design code developed at MIT for the US Navy [2], based on lifting line theory. Its strength is that unlike the Reynolds-Averaged Navier-Stokes (RANS) methods used in most commercial CFD, it has the ability to optimize the circulation distribution along a propeller blade. This particular version of PLL also supports ducted designs with multiple rotors[2].

[2]Propeller Vortex Lattice (PVL) is a similar open-source code available at http://ocw.mit.edu/OcwWeb/Mechanical-Engineering/2-23Fall-2003/Assignments/index.htm in the supporting files for homework 9

TABLE II

PROPULSOR SUMMARY AT DESIGN POINT

Inflow Velocity, U_in [m/s]	1.0
Thrust, T [N]	21.17
Efficiency, η	0.572
Shaft Torque, Q_s [mN-m]	189.8

The code solves for the circulation matrix and performs multiple iterations, accounting for the interactions between all the bound vortices on the propellers and the free vortices in the wake. Quickly converging solutions ($<$ 25 iterations) are generally a good indication of reliable results.

Since lifting line codes have no provisions for viscosity, they cannot predict stall. Every output must be inspected for realistic 2-D sectional lift coefficients to prevent backflow near the hub of the propeller. If backflow is present, the hub diameter should be increased sufficiently to eliminate it. Generally, a hub diameter of 20% the propeller diameter is sufficient in marine propellers.

C. Design Operating Point

It is obvious from Figure 2 that larger diameter propulsors have higher potential efficiencies, so it was expected that our design operating point would be the largest the vehicle could accommodate, 11.43 cm. This corresponds to a relatively high thrust coefficient: $C_T = 3.8$. One of the motors we were investigating fit the requirements almost perfectly. It was available with a high-quality factory gearbox at an appropriate gear ratio, and the continuous permissible torque (based on recommended thermal limits) was right at the expected design point. As illustrated in Figure 3, six-bladed propellers offers a slight increase in efficiency over three-bladed propellers. However, this is at a higher advance coefficient (meaning lower motor speed) and higher torque. Since our design is for 12V DC motors at 6 amps, it is advantageous for us to choose the 3-bladed design at a higher motor speed. The characteristics of the propulsor optimized for that operating point are summarized in Table II

III. PROPELLERS & DUCT DESIGN

A. 3-D Convergence

Lifting Line theory is a good tool for determining the optimum design point for a particular propulsor, and for giving the designer a good starting geometry. However, a more advanced method should be used to fully capture the three-dimensional effects of the flow and tweak the final geometry. PBD 14.36 [3] is a 3D vortex lattice code designed for just that. It is generally coupled with RANS solver, like MTFLOW [4]. This coupled solver is iterated until a stable solution is found, defining the fine three-dimensional geometry of each propeller, along with the axisymmetric offsets of the duct.

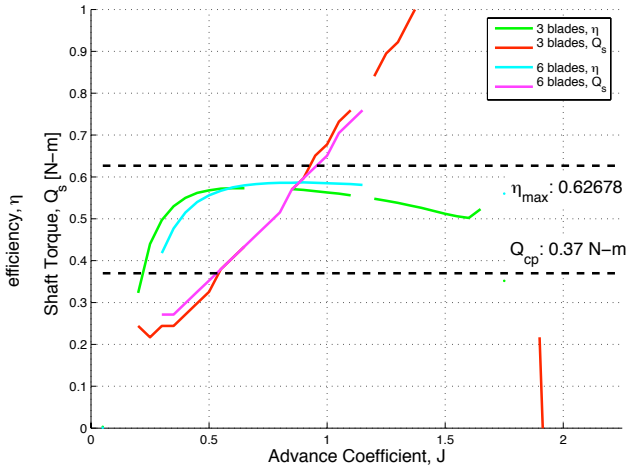

Fig. 3. Choosing the operating point for the DCRP-2006, C_T = 3.8 and D = 11.43 cm. The maximum possible efficiency from actuator disk theory and the continuous torque rating of the Maxon RE40 with its gearbox are provided for reference. Note that the six-bladed design has slightly higher possible efficiencies, but at the expense of higher torque and advance coefficient.

1) Blade Shape Convergence: PBD examines the flow field and displaces a number of vertices on the b-spline surface representing the mean camber surface of the blade. MTFLOW solves the flow field with the new propeller geometry, and the two iterate until the vertex displacement becomes negligible. In multi-component propulsors (like our contrarotating propeller set, a matched propeller-stator combination, or a waterjet) PBD is run separately on each component before MTFLOW solves the flowfield. The coupled PBD-MTFLOW solution usually takes 3-6 iterations if a good output from PLL is used.

2) Duct Geometry: In addition to converging the blade shape, PBD allows the designer to examine different duct geometries. The boundaries of the flow field are defined for MTFLOW in a text file. A section of that file describes the outline of the duct. The chord, camber, angle of attack, and thickness of the duct need to be varied systematically in order to find a duct geometry that will yield the duct loading, τ, solved for in the parametric study. Once blade shape has converged, an MTFLOW utility is used to evaluate the thrust contributed by each section of the flow field. Comparing the total thrust to the duct thrust gives an expression for τ:

$$\tau = 1 - \frac{T_{duct}}{T_{total}}. \tag{5}$$

The final duct geometry for DCRP-2006 is listed in Table III. The thickness profiles used is a modified NACA66 where the trailing edge has been thickened for strength purposes. It is combined with the NACA $a = 0.8$ camber line commonly used in marine propeller sections [8].

3) Velocity Fields: MTFLOW solves the entire flow field with each iteration of the coupled solution. It is helpful to inspect the velocity field around the propulsor at each iteration. It is important in ducted designs to inspect the streamlines at the leading edge of the duct, making sure to avoid separation

TABLE III
PHYSICAL ATTRIBUTES OF THE DUCT

Duct loading, τ	0.6 - 1.0
Diameter, D [cm]	13.97
Chord, c [cm]	13.97
Thickness, t_0/c	0.111111
Camber, f_0/c	-0.0237
Angle of Attack, α	5.875°
tip gap (rear propeller) [cm]	0.1588

there. It is also useful to look at the overall tangential velocity field to see that swirl is restricted to the space between the two propellers of a contrarotating design(see Figure 4(b)).

B. Fabrication

Perhaps the most challenging part of this project was the actual fabrication of the propellers. We originally planned on using a 3-D printer to make molds. These would either be printed directly, or soft molds would be poured around a 3-D printed original. Due to monetary and time constraints, and to difficulties in fully resolving the complex propeller geometry in a CAD program, we ultimately gave up on the printing idea. We plan to pursue it further in the future.

The propellers were instead CNC milled directly from solid blanks of polypropylene. Extra thickness was added to the blades when it became apparent that our original design would be too weak using this material. The machining required custom-made jigs to ensure the two sides of the propeller would match up. The end result was not as true to our hydrodynamic design as we would have preferred, but it served us well in these prototype thrusters and at the MATE ROV Competition.

IV. MECHANICAL SYSTEM DESIGN

Contrarotating designs are traditionally realized by coaxial, contrarotating shafts. These mechanisms introduce significant complexity into the system, especially in miniaturization and waterproofing. Furthermore, the gearing required to achieve contrarotation introduces another level of mechanical loss and another potential failure point for the propulsor. It was very important to our design to minimize complexity and keep repairs and maintenance simple, so other methods were explored.

A. Contrarotating Gearbox

After investigating many possible solutions, a custom 1:1 miter gearbox was chosen as the method to achieve contrarotation. In order to minimize complexity in the shaft seals, this gearbox operates wet. It is located at the front of the propeller assembly, just behind the forward stator. The motor delivers power to one common shaft that serves to support and align both propellers. The rear propeller is driven directly by this shaft, and the forward propeller floats on this shaft, held by Rulon bearings and driven by the miter gearbox. In a mirror-image, the forward miter gear is driven by the shaft and power is transmitted through the freewheeling side gears to the rear miter gear, which is press-fit into the hub of the forward propeller. The entire miter gearbox fits within the 2.54 cm (1 in) diameter hub of the propulsor to limit any hydrodynamic interference with the propellers. The gearbox housing is Acetal copolymer, the miter gears are nylon, and the shaft is stainless steel; all materials were chosen to provide low friction and good corrosion resistance, since any fouling in the gearbox could negate the efficiency gain of the contrarotating propellers.

B. Stators & Duct

The propulsor is surrounded by a duct to increase hydrodynamic performance and help keep debris from fouling on the propellers. The duct was turned on a CNC lathe from solid polypropylene stock to minimize weight and cost while ensuring hydrodynamic accuracy. It is mounted to the propulsor using three-leg stators of polycarbonate. Standoffs were incorporated in the design to provide additional axial space for the contrarotating gearbox.

Fig. 5. CAD model of DCRP-2006 with contrarotating miter gearbox (enlarged at left) highlighted in green. The contrarotating miter gearbox is run wet to simplify sealing, assembly, and maintenance.

C. Motor & Housing

We chose the Maxon RE40 DC brush motor (www.maxonmotor.com) to power the DCRP-2006. It was one of the only motors available with 12V windings in the power range we required, and a stock planetary gearbox was available that would reduce it to our operating range.

It is housed in a thin aluminum casing with Acetal copolymer endcaps. The casing is turned on a CNC lathe to such precision that the stickers on the body of the motor must be removed for it to fit. This close-fit is important because it heat-sinks the motor to the surrounding water, extending the continuous operating range of the propulsor. The endcaps have double o-ring static seals. Power is transmitted through an Impulse Enterprises (www.impulse-ent.com) wet-pluggable bulkhead connector on the forward endcap. The shaft penetrates the hydrodynamically-faired rear endcap and is sealed with a Parker Flexi-Seal spring-loaded PTFE o-ring (www.parker.com). This shaft seal is especially well-suited to

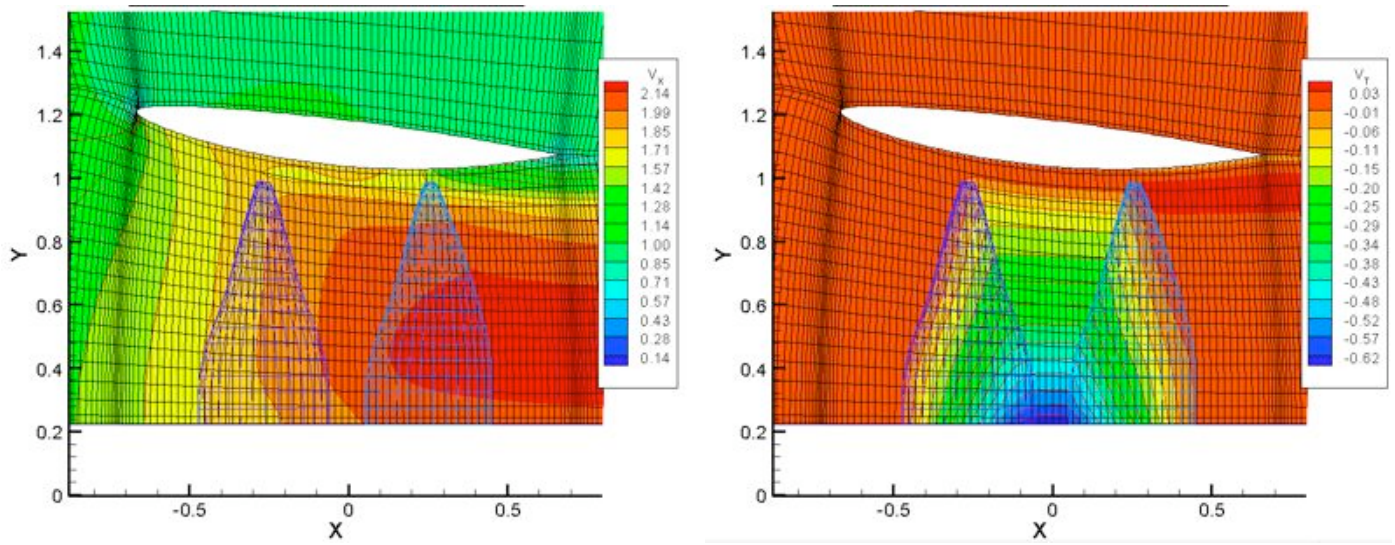

(a) Axial velocity

(b) Tangential velocity; note the cancellation of swirl

Fig. 4. Axisymmetric velocity fields modeled by PBD14.36 and MTFLOW. Axes are nondimensionalized by propeller diameter. Velocities are given in meters per second. Note the fine mesh near the leading and trailing edges where flow resolution is important to observe and avoid stall.

high rotation rate applications and operates with minimum frictional losses.

V. Propulsion Tests

We performed propulsion tests on the DCRP-2006 to evaluate how well our prototypes perform in controlled conditions. Standard propulsion curves were generated from data collected in the recirculating water tunnel at the MIT Marine Hydrodynamics Laboratory (Figure 6).

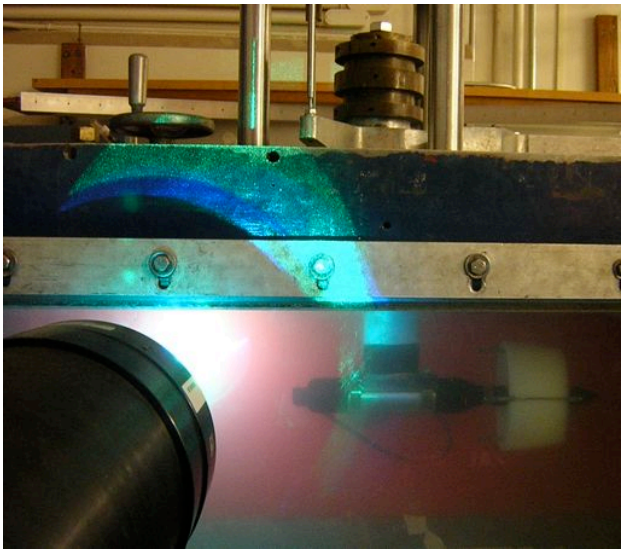

Fig. 6. DCRP-2006 undergoing propulsion tests in the MHL recirculating water tunnel. A six-axis dynamometer (on the top window) measures forces transmitted through the streamlined strut holding the propulsor. Mean inflow is determined by Laser Doppler Velocitmetry (LDV), the barrel of the laser is to the left.

A. Experimental Setup

The tunnel test section is 1.2 meters long by 50 cm square through which an extremely uniform stream of water can be moved at speeds up to 10 m/s. Force and current measurements were recorded at 100 Hz using a LabVIEW data acquisition system. Thrust was measured using a Lebow load cell (www.lebow.com), and electrical current was recorded using an open loop hall effect current sensor (www.sypris.com). Propeller rotation rate was measured using a strobe, since the DCRP-2006 is not equipped with a tachometer or an encoder. Mean inflow velocity was measured using Laser Doppler Velocimetry (LDV).

B. Results

Data was collected at inflow speeds of 0.85, and 1.0 m/s. The rotation rate was varied from 600 RPM to 1100 RPM for each inflow speed. Thrust and current were averaged over test intervals of not less than 15 seconds. Each test was conducted three times and the results were averaged. Torque was estimated using the current measurements and known properties of the motor and gearbox. Data was then nondimensionalized to produce K_T, K_Q, and η curves, displayed in Figure 7. Linear fits were applied to the data for K_T and K_Q, a third-order fit was used for η.

The measured current gave a higher torque than predicted by PLL. That was expected, however, due to losses in power transmission ot the thruster, unaccounted losses in the contrarotating miter gearbox, and the rough cut of the actual propellers. Considering all these factors, the experimental data is very close to the expected performance of the thruster. This provides validation to the design of DCRP-2006, and the data will also be used to provide an accurate thrust map for the MIT ROV that will enhance the current control algorithms.

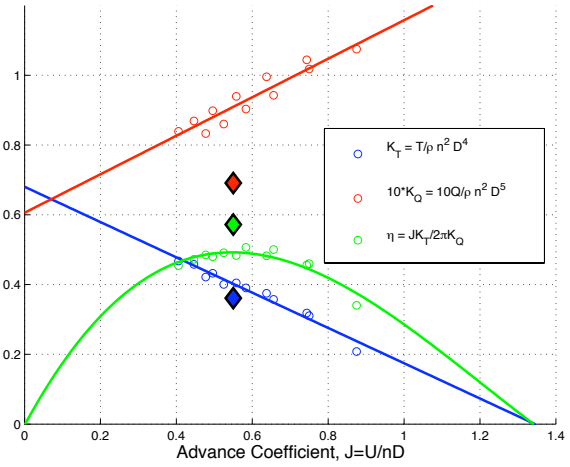

Fig. 7. Propulsion curves for DCRP-2006. Linear fits are applied to K_T and K_Q, and a third-order fit is applied to η. Residuals from these fits were less than 0.04. The values predicted by PLL at the design operating point are shown by diamonds.

Fig. 8. The MIT ROV handling a large payload (red & black) in the big pool at NASA's Neutral Buoyancy Lab (Houston, TX). This mission taught us that protective grilles are required if we plan on using these propulsors on an ROV with a fiber optic tether.

VI. Conclusion

To evaluate the performance of our prototypes in real-world conditions, four DCRP-2006 propulsors were installed on the MIT ROV. They worked well in the competition and will continue to serve the team in the future. The propulsion tests provided validation of the design tools used in this project, and it is hoped that more precise propellers can be made in the future to provide even stronger validation.

VII. Future Work

The first priority in improving these propulsors is integrating a protective grille on both sides of the duct. The suction produced at the DCRP-2006 intake is sufficient to draw many things into the propellers. Debris may damage the blades or the interior of the duct, but the impetus for this improvement comes mainly from the fiber optic tether used by the MIT ROV Team. During a competition run, it was pulled into the propulsor, wound around the hub, and eventually broken, severing communications with the robot while it was still submerged.

Another area that should be developed further is making more accurate propellers. Developing the ability to 3-D print molds or originals would greatly simplify the whole design cycle and speed up manufacturing.

Another type of experiment that can be performed on the propulsors, and is planned for the future, is using particle image velocimetry (PIV) to visualize the wake and confirm that the end product cancels swirl as effectively as predicted.

Acknowledgment

The authors would like to thank everyone who helped us throughout this project. Prof. Jake Kerwin and Dr. Rich Kimball for supplying the codes, teaching us how to use them, and general advice, Prof Alex Techet and Dr. Franz Hover for being supportive advisors throughout, Mr. Thad Michaels, NSWCCD, for his assistance in preparing our files for CAD, and the MIT ROV Team (especially Dan and Eddie for lots of machining), the Edgerton Center, the MIT Towing Tank, and the MIT Marine Hydrodynamics Lab for offering time and resources. We could not have done it without your support.

References

[1] J. E. Kerwin, *13.04 Lecture Notes: Hydrofoils and Propellers*. Cambridge, MA: Massachusetts Institute of Technology, 2001.

[2] W. B. Coney, C.-Y. Hsin, and J. E. Kerwin, *A Vortex Lattice Lifting Line Program for Single and Multi-Component Propulsors*. Cambridge, MA: MIT Department of Ocean Engineering, 1986.

[3] A. Chrisospathis, J. E. Kerwin, and T. E. Taylor, *PBD 14.36: A Coupled Lifting-Surface Design/Analysis Program for Marine Propulsors*. Cambridge, MA: MIT Department of Ocean Engineering, 2001.

[4] M. Drela, *A User's Guide to MTFLOW 1.1: Multi-passage ThroughFLOW Design/Analysis Program*. Cambridge, MA: MIT Fluid Dynamics Research Laboratory, 1997.

[5] J. E. Kerwin, *The Preliminary Design of Advanced Propulsors*. Presented at Propellers/Shafting '03 Symposium, Virginia Beach, VA. September 16-17, 2003. Society of Naval Architects and Marine Engineers (SNAME).

[6] B. Y.-H. Chen, and A. M. Reed, *A Design Method and Application for Contrarotating Propellers*. Bethesda, MD: David Taylor Research Center, 1990.

[7] B. Y.-H. Chen, and C. L. Tseng, *A Contrarotating Propeller Design for a High Speed Patrol Boat with Pod Propulsion*. Bethesda, MD: Naval Surface Warfare Center - Carderock Division, 1995.

[8] T. Brockett, *Minimum Pressure Envelopes for Modified NACA-66 Sections with NACA a=0.8 Camber and Buships Type I and Type II Sections*. Bethesda, MD: David Taylor Research Center, 1966.

[9] *LBV150-2 Specifications*. http://www.seabotix.com/products/lbv150_specifications.htm, Seabotix, Inc. viewed 01 February, 2006.

[10] *Remus 100*. http://www.hydroidinc.com/remus100.html, Hydroid, LLC. viewed 01 February, 2006.